Electronic Supplementary Material (ESI) for CrystEngComm.

<Electronic Supplementary Information>

In situ crystalline transformation of bis(halo)mercury(II) coordination polymers to ionic chloro-bridged-bis(halo)mercury(II) species via UV irradiation in chloroform media

Eunkyung Choi, Haeri Lee, Tae Hwan Noh and Ok-Sang Jung*

Department of Chemistry, Pusan National University, Busan 46241, Korea.

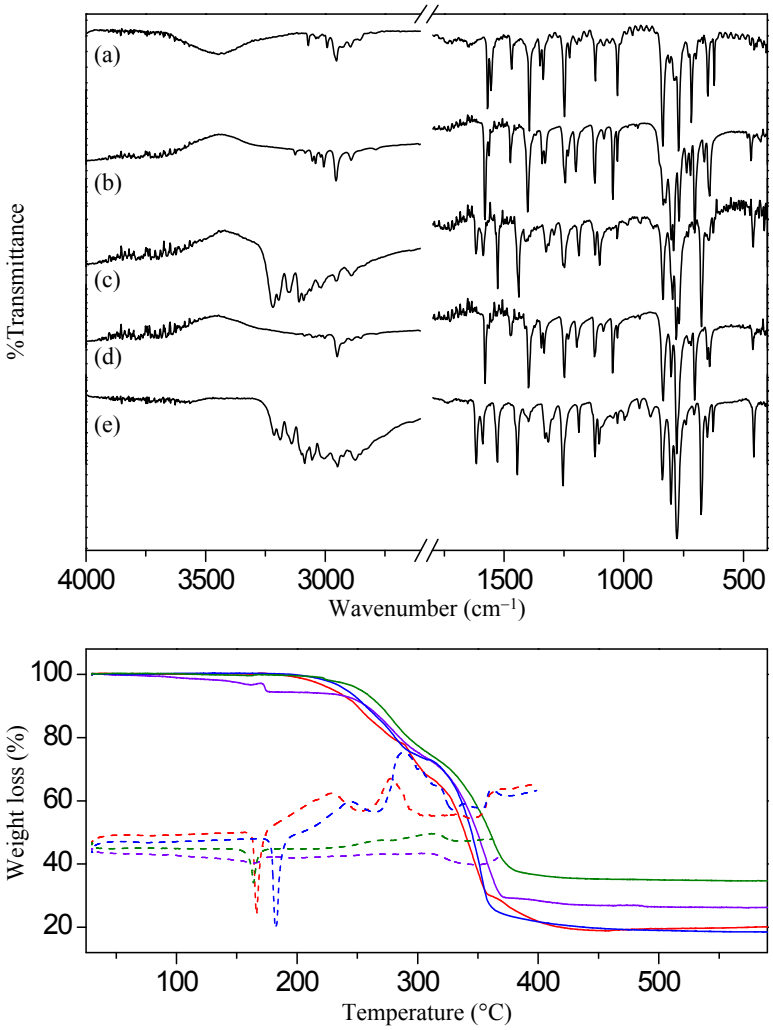

Fig. S1 Top: IR spectra of L (a), $[HgBr_2L]$ (b), $[H_2L]^{2+}[Hg_2Br_4(\mu\text{-}Br)(\mu\text{-}Cl)]^{2-}$ (c), $[HgI_2L]$ (d), and $[H_2L]^{2+}[HgI_2(\mu\text{-}Cl)]_2^{2-}$ (e). Bottom: TGA (solid lines) and DSC (dashed lines) curves of $[HgBr_2L]$ (red), $[H_2L]^{2+}[Hg_2Br_4(\mu\text{-}Br)(\mu\text{-}Cl)]^{2-}$ (purple), $[HgI_2L]$ (blue), and $[H_2L]^{2+}[HgI_2(\mu\text{-}Cl)]_2^{2-}$ (green).

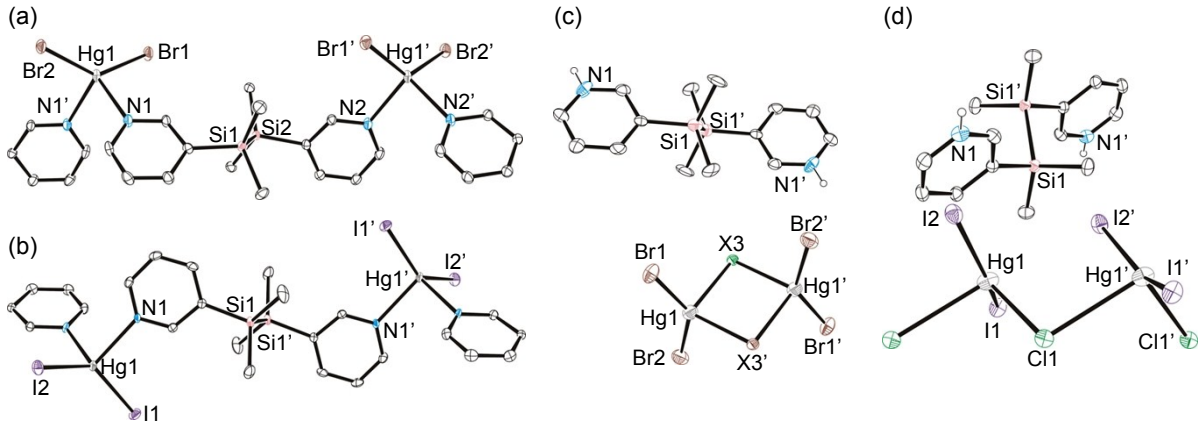

Fig. S2 ORTEP drawings with anisotropic displacement parameters at 30% probability of $[HgBr_2L]$ (a), $[HgI_2L]$ (b), $[H_2L]^{2+}[Hg_2Br_4(\mu\text{-Br})(\mu\text{-Cl})]^{2-}$ (c), and $[H_2L]^{2+}[HgI_2(\mu\text{-Cl})]_2^{2-}$ (d). Hydrogen atoms (except for N–*H*) were omitted for clarity. In (c), the atoms X(3) and X(3') are both chloride and bromide anions with the occupancies of 50 : 50.

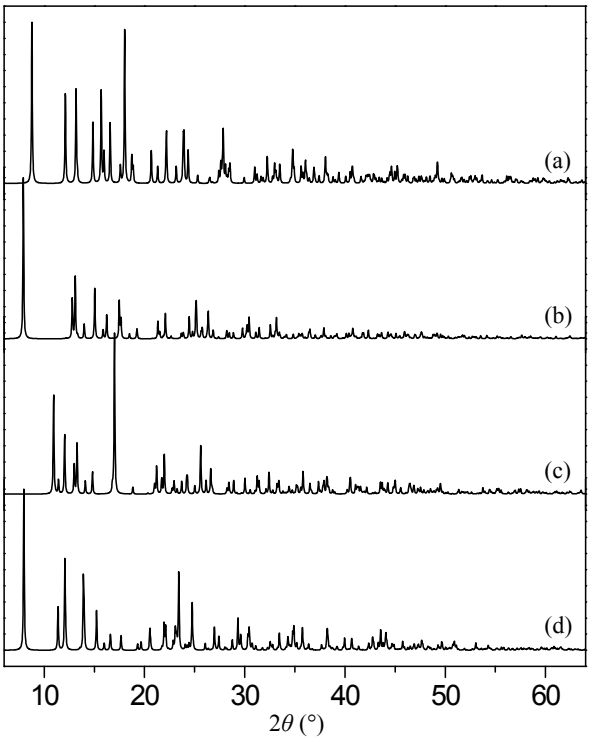

Fig. S3 Powder XRD patterns of $[HgBr_2L]$ (a), $[H_2L]^{2+}[Hg_2Br_4(\mu\text{-}Br)(\mu\text{-}Cl)]^{2-}$ (b), $[HgI_2L]$ (c), and $[H_2L]^{2+}[HgI_2(\mu\text{-}Cl)]_2^{2-}$ (d).

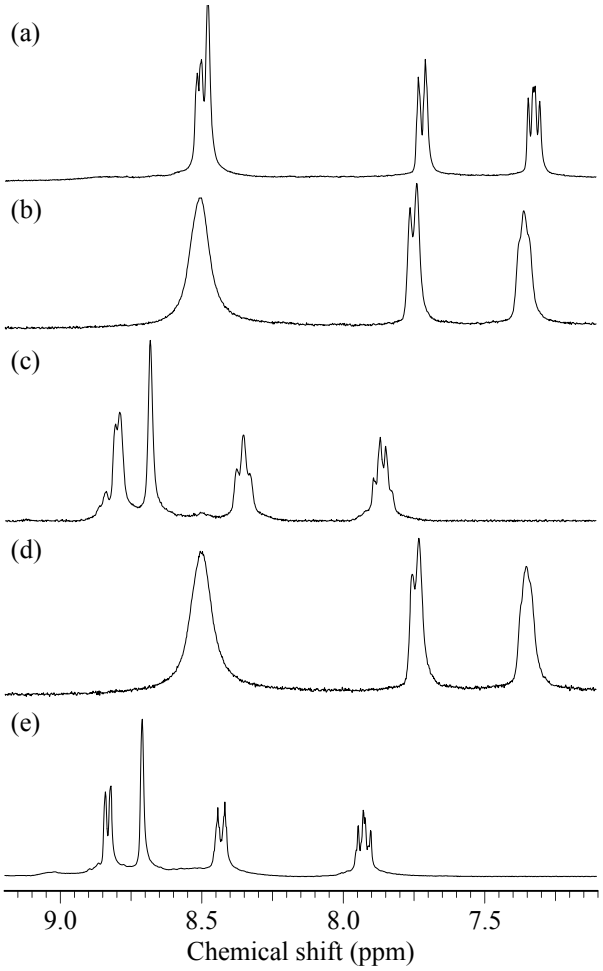

Fig. S4 Partial ^{1}H NMR spectra (Me_2SO-d_6) of L (a), $[HgBr_2L]$ (b), $[H_2L]^{2+}[Hg_2Br_4(\mu\text{-}Br)(\mu\text{-}Cl)]^{2-}$ (c), $[HgI_2L]$ (d), and $[H_2L]^{2+}[HgI_2(\mu\text{-}Cl)]_2^{2-}$ (e).

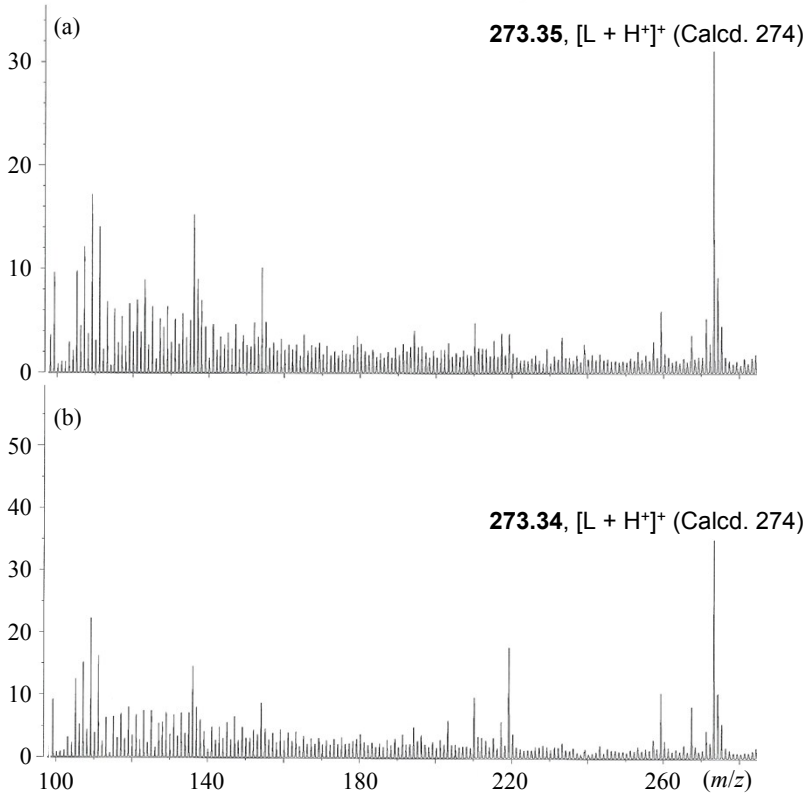

Fig. S5 FAB-Mass data for the resulting chloroform solution of $[HgBr_2L]$ (a) and $[HgI_2L]$ (b) after UV-irradiation for 8 h.

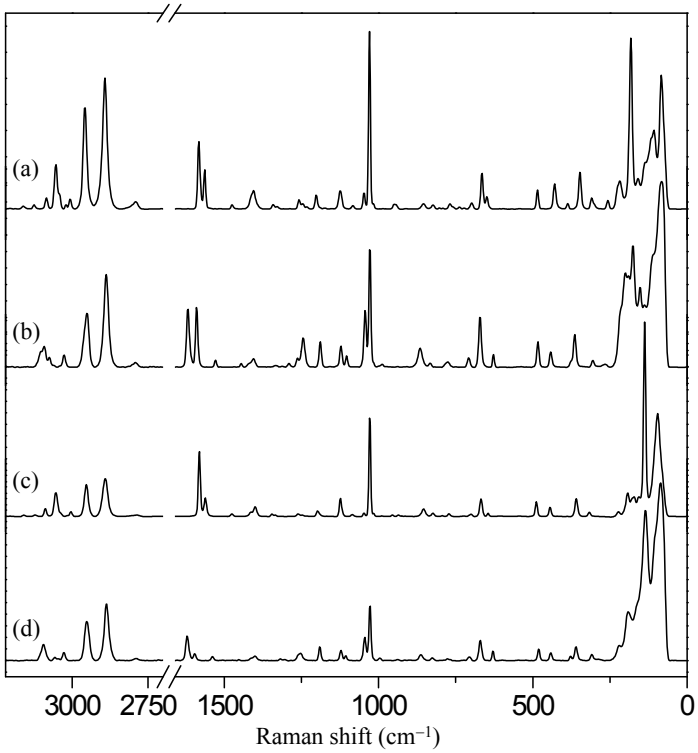

Fig. S6 Full Raman spectra of $[HgBr_2L]$ (a), $[HgI_2L]$ (b), $[H_2L]^{2+}[Hg_2Br_4(\mu\text{-Br})(\mu\text{-Cl})]^{2-}$ (c), and $[H_2L]^{2+}[HgI_2(\mu\text{-Cl})]_2^{2-}$ (d).

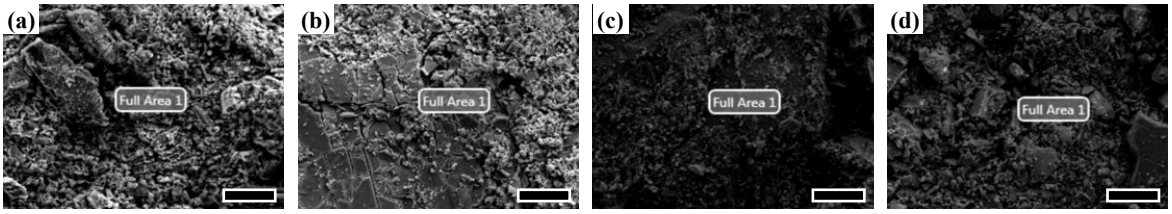

	(a)		(b)		(c)		(d)	
	Atomic%	Error%	Atomic%	Error%	Atomic%	Error%	Atomic%	Error%
C	65.33	10.47	56.8	11.15	62.67	8.88	56.98	9.78
N	11.99	16.92	6.79	21.87	7.97	16.93	6.96	19.45
Si	9.61	5.7	7.75	6.71	10.59	5.91	7.26	6.43
Hg	5.07	2.88	8.28	2.38	6.04	3.34	7.46	3.15
Cl	–	–	5.71	6.79	–	–	8.04	5.55
Br	7.93	2.36	13.05	3.05	0.27	3.4	0.22	20.44
I	0.07	57.56	1.61	12.93	12.46	20.15	13.08	3.49

Fig. S7 SEM-EDX data of $[HgBr_2L]$ (a), $[H_2L]^{2+}[Hg_2Br_4(\mu\text{-}Br)(\mu\text{-}Cl)]^{2-}$ (b), $[HgI_2L]$ (c), and $[H_2L]^{2+}[HgI_2(\mu\text{-}Cl)]_2^{2-}$ (d). Bar = 50 μm.

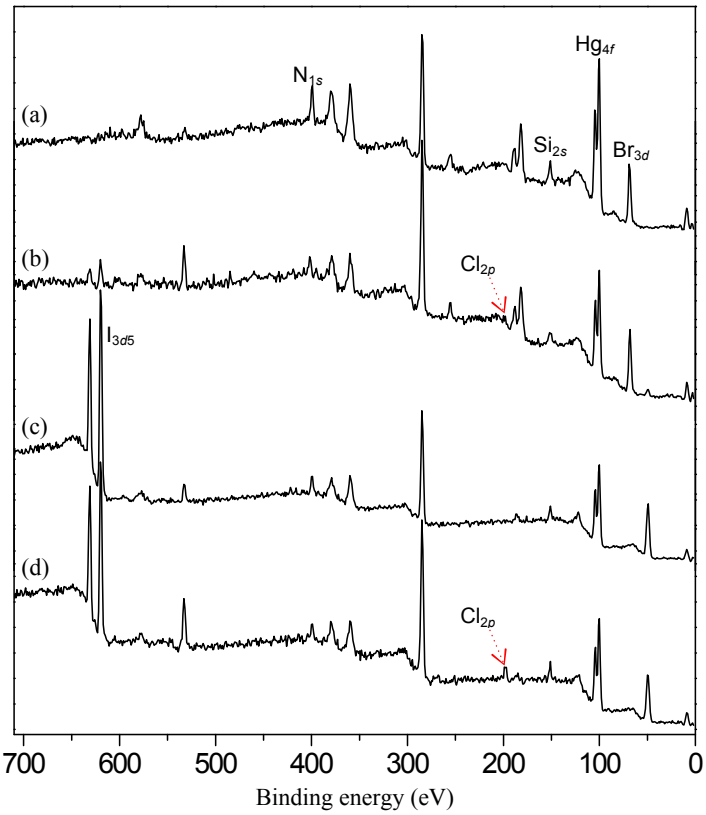

Name	Atomic%
Hg_{4f}	4.43
Si_{2s}	9.58
Br_{3d}	8.82

Name	Atomic%
Hg_{4f}	2.62
Si_{2s}	5.40
Br_{3d}	7.16
Cl_{2p}	1.61

Name	Atomic%
Hg_{4f}	3.41
Si_{2s}	10.28
I_{3d5}	7.81

Name	Atomic%
Hg_{4f}	2.57
Si_{2s}	6.86
I_{3d5}	5.61
Cl_{2p}	3.01

Fig. S8 Full XPS spectra and the atomic% values of $[HgBr_2L]$ (a), $[H_2L]^{2+}[Hg_2Br_4(\mu\text{-}Br)(\mu\text{-}Cl)]^{2-}$ (b), $[HgI_2L]$ (c), and $[H_2L]^{2+}[HgI_2(\mu\text{-}Cl)]_2^{2-}$ (d).